A Protective Effect of PPARα in Endothelial Progenitor Cells Through Regulating Metabolism

Yan Shao,[1,2,3] Jianglei Chen,[3] Li-jie Dong,[1,3] Xuemin He,[3] Rui Cheng,[3] Kelu Zhou,[3] Juping Liu,[1] Fangfang Qiu,[3] Xiao-rong Li,[1,2] and Jian-xing Ma[3,4]

Diabetes 2019;68:2131–2142 | https://doi.org/10.2337/db18-1278

Deficiency of endothelial progenitor cells, including endothelial colony-forming cells (ECFCs) and circulating angiogenic cells (CACs), plays an important role in retinal vascular degeneration in diabetic retinopathy (DR). Fenofibrate, an agonist of peroxisome proliferator–activated receptor α (PPARα), has shown therapeutic effects on DR in both patients and diabetic animal models. However, the function of PPARα in ECFC/CACs has not been defined. In this study, we determined the regulation of ECFC/CAC by PPARα. As shown by flow cytometry and Seahorse analysis, ECFC/CAC numbers and mitochondrial function were decreased in the bone marrow, circulation, and retina of *db/db* mice, correlating with PPARα downregulation. Activation of PPARα by fenofibrate normalized ECFC/CAC numbers and mitochondrial function in diabetes. In contrast, *PPARα* knockout exacerbated ECFC/CAC number decreases and mitochondrial dysfunction in diabetic mice. Primary ECFCs from *PPARα*$^{-/-}$ mice displayed impaired proliferation, migration, and tube formation. Furthermore, *PPARα*$^{-/-}$ ECFCs showed reduced mitochondrial oxidation and glycolysis compared with wild type, correlating with decreases of Akt phosphorylation and expression of its downstream genes regulating ECFC fate and metabolism. These findings suggest that PPARα is an endogenous regulator of ECFC/CAC metabolism and cell fate. Diabetes-induced downregulation of PPARα contributes to ECFC/CAC deficiency and retinal vascular degeneration in DR.

Diabetic retinopathy (DR) is the leading cause of visual disability in the working-age population (1). Chronic hyperglycemia, dyslipidemia, and hypoxia are believed to impair microvasculature (2).

Endothelial progenitor cells (EPCs) are believed to play an important role in retinal vascular repair (3). EPCs are a rare population of bone marrow (BM)–derived circulating cells that were first discovered by Asahara et al. in 1999 (4) and can develop endothelial phenotypes in vitro. However, recent studies revealed that there are at least two subsets of EPCs: circulating angiogenic cells (CACs) and endothelial colony-forming cells (ECFCs); the latter are considered true EPCs due to the capability of integrating directly into the developing vessels and forming tubelike structure in vitro (5) and providing promising therapeutic potential (6). Although CACs are not endothelial progenitors, they play an important proangiogenic role and can be used as a biomarker in a number of diseases. Hence, both of these subtypes of EPCs are involved in the pathogenesis of DR (7). Continuous controversy exists in the definition and characterization of termed EPCs, not only in the human but also in the mouse (8). However, both CACs and ECFCs have been demonstrated to contribute to vascular repair via postnatal vasculogenesis, either through paracrine angiogenic effects (CACs) or directly via integration into new blood vessels (ECFCs). Under diabetic conditions, EPC numbers were changed, and their functions were dysregulated (7), leading to impaired vascular repair and progression of microvascular pathologies.

Fenofibrate has displayed robust therapeutic effects on diabetic microvascular complications such as DR, as

[1]Eye Institute and School of Optometry, Tianjin Medical University Eye Hospital, Tianjin, China
[2]Tianjin Key Laboratory of Retinal Functions and Diseases, Eye Institute and School of Optometry, Tianjin Medical University Eye Hospital, Tianjin, China
[3]Department of Physiology, The University of Oklahoma Health Sciences Center, Oklahoma City, OK
[4]Harold Hamm Diabetes Center, The University of Oklahoma Health Sciences Center, Oklahoma City, OK

Corresponding author: Xiao-rong Li, xiaorli@163.com, or Jian-xing Ma, jian-xing-ma@ouhsc.edu

Received 4 December 2018 and accepted 23 August 2019

This article contains Supplementary Data online at http://diabetes.diabetesjournals.org/lookup/suppl/doi:10.2337/db18-1278/-/DC1.

reported independently by two large, longitudinal clinical studies: Fenofibrate Intervention and Event Lowing in Diabetes (FIELD) (9) and Action to Control Cardiovascular Risk in Diabetes (ACCORD) (10). The therapeutic effects of fenofibrate on DR have been ascribed to its anti-inflammatory, antiapoptotic, antioxidative, and antiangiogenic activities in diabetic conditions (11). Recently, Deng et al. (12) reported that fenofibrate also showed protective effects on EPCs in a diabetic mouse model and accelerated skin wound healing via inhibition of inflammation pathways.

Fenofibrate belongs to the fibrate family, and its active metabolite, fenofibric acid, is an agonist of peroxisome proliferator–activated receptor α (PPARα) (13). PPARs regulate lipid metabolism and glucose homeostasis (14). Our previous studies identified the role of PPARα in direct transcriptional control of fatty acid oxidation (FAO) genes involved in the mitochondrial β-oxidation pathways (15). Furthermore, excessive fatty acid storage causes insulin resistance (16), which is characterized by an impaired ability of insulin to promote glucose uptake in target tissues. PPARα activation in obese mice has been reported to improve insulin sensitivity and decrease blood glucose (17). Mitochondria dysfunction (18) and insulin resistance (19) can cause EPC dysregulation in disease conditions.

It has been reported that PPARα activation protects myocardium from ischemia-reperfusion injury via the activation of the PI3K/Akt pathway (20,21), and downregulation of Akt activity contributes to EPC dysfunction in diabetic conditions (20,22). Meanwhile, the Akt pathway shows beneficial effects on glucose and lipid metabolism in diabetes (23). Accumulating scientific evidence identified PPARα as the nexus of mitochondrial oxidation and glycolysis in metabolism pathways. Although fenofibrate has shown therapeutic effects on diabetic microvascular complications clinically (24,25), the crucial link between PPARα and ECFC/CAC fate under diabetic conditions and the underlying mechanism has not been documented.

The current study investigated the regulatory role of PPARα in ECFC/CAC function and cell fate through metabolism control. This study demonstrated that diabetes-induced downregulation of PPARα is responsible for the impaired mitochondrial function of ECFC/CACs, suggesting a potential therapeutic target for vascular damage in diabetes and other metabolism-related disorders.

RESEARCH DESIGN AND METHODS

Animals

Male *db/db* mice and their heterozygous littermates in the C57BLKS/J background were purchased from The Jackson Laboratory (Bar Harbor, ME). At 8 weeks of age, the mice were randomly assigned into two groups: one fed regular chow as control and the other fed special chow containing 0.014% fenofibrate (LabDiet; TestDiet, Fort Worth, TX) for another 12 weeks.

Streptozotocin-Induced Diabetic Animal Model

Eight-week-old male *PPARα*$^{-/-}$ mice and genetic background- and age-matched wild-type (WT) C57BL/6J mice (The Jackson Laboratory) received daily intraperitoneal injections of streptozotocin (STZ) at a dose of 55 mg/kg for 5 consecutive days. Animals with blood glucose levels >350 mg/dL were defined as diabetic animals.

All of the animal experiments were approved by the Institutional Animal Care and Use Committee of The University of Oklahoma.

Mouse ECFC Isolation and Culture

Mouse ECFCs were isolated and cultured following documented protocols (26,27). To minimize variations caused by the circadian cycle, BM cells were isolated from the femurs and tibias of mice at age postnatal day 28 (P28) in the morning and one from each group alternatively. Briefly, the mononuclear cells were collected by density-gradient centrifugation using Histopaque 1083 (Sigma-Aldrich, St. Louis, MO) and plated on dishes precoated with collagen (1 μg/mL) and cultured in EGM-2 using the EGM-2 bullet kit, containing 10% FCS (Lonza, Basel, Switzerland). After 14 days, the ECFCs were identified by immunofluorescence staining using Dil-conjugated acetylated LDL and FITC–UEA-I (Supplementary Fig. 1). All further in vitro studies used subcultured ECFCs in the passage of P1.

FACS Analysis

To quantify the ECFC/CAC population in vivo, FACS was used as previously described (28). Samples were transferred into 12 75-mm polystyrene round-bottom tubes and incubated with CD45-FITC (103108; BioLegend, San Diego, CA), CD133-PE (141204; BioLegend), CD34-BV421 (119321; BioLegend), and VEGFR2-APC (136406; BioLegend) antibodies for 1 h in the dark. The red blood cells were lysed by adding 2 mL of RBC Lysing Buffer (BD Biosciences, Franklin Lakes, NJ) per sample for 15 min. The samples were measured by Stratedigm S1300Ex (Stratedigm, Inc., San Jose, CA). Because both ECFCs (CD45^{-}) and CACs (CD45^{dim}) contribute to postnatal angiogenesis, CD34^{+}, VEGFR2^{+}, CD45$^{-/dim}$, and CD133^{+} populations in BM, circulation, and retina were analyzed by FlowJo software (Life Science Software Company, Ashland, OR).

Mitochondrial Membrane Potential

Mitochondrial membrane potential ($\Delta\Psi_m$) of the CD34^{+}, VEGFR2^{+}, and CD45$^{-/dim}$ population, including both ECFCs (CD45^{-}) and CACs (CD45^{dim}), was estimated using flow cytometry (FCM) and fluorescent probe JC-1 (5,5′,6,6′-tetrachloro-1,1′,3,3′-tetraethylbenzimidazolcarbocyanine iodide) (551302; BD Biosciences). Samples were collected using FACS as previously described and then immunolabeled with CD45-BV605 (103139; BioLegend), CD34-BV421 (119321; BioLegend), and VEGFR2-APC

(136406; BioLegend) antibodies for 1 h. Samples were stained with 2.5 μmol/L JC-1 at 37°C for 15 min and analyzed by FCM immediately.

Metabolic Function Evaluation

The retinas were dissected, punched at 1.5 mm from the optic nerve to obtain a retinal biopsy of 1 mm in diameter, and analyzed using a Seahorse XFe96 Flux Analyzer (Agilent Technologies, Santa Clara, CA) as previously described (15).

To obtain simultaneous measurement of cell-mitochondrial respiration and glycolysis, the Seahorse XFe96 Cell Energy Phenotype Test Kit was used (Agilent Technologies) following the manufacturer's instructions.

Electroretinography Recording

Electroretinography (ERG) was recorded using the Diagnosys Espion Visual Electrophysiology System (Diagnosys LLC, Lowell, MA) as described previously (29). For scotopic ERG, mice were dark-adapted for 16 h. The flash intensity was 600 cds/m^2 for scotopic ERG. The ERG responses of both eyes were simultaneously recorded and analyzed.

In Vitro Tube Formation Assay

ECFCs (2×10^4 cells/well) were seeded to Matrigel (BD Biosciences) precoated 96-well plates and incubated for 10 h. The enclosed networks of tubes were photographed from six random fields under a microscope. The average tube length was measured and compared by Image-Pro Plus (Media Cybernetics, Inc., Rockville, MD).

Cell Migration Assay

The migratory function of ECFCs was analyzed by a modified Boyden chamber (CoStar, Cambridge, MA) assay following the manufacturer's protocol. Briefly, 1×10^5 ECFCs were placed in the upper chamber, and a medium containing 20% FBS was placed in the lower chamber, followed by a 16-h incubation at 37°C in 5% CO_2. After washes and fixation, the migrated ECFCs on the bottom were stained with DAPI and counted in six random high-power (×40 magnification) microscope fields per well.

Cell Proliferation Assay

ECFCs were seeded onto a 96-well plate (2×10^4 cells/well), and cell proliferation was analyzed using the BrdU incorporation ELISA kit (ab126556; Abcam, Cambridge, MA) following the manufacturer's instructions.

Western Blot Analysis

The equal amount of protein was resolved and immunoblotted with primary antibodies for Nrf1 (NBP1-89125; Novus Biologicals, Littleton, CO), Nrf2 (NBP1-32822; Novus Biologicals), sirtuin 1 (Sirt1) (D1D7-9475; Cell Signaling Technology, Danvers, MA), Glut1 (SC-7903; Santa Cruz Biotechnology, Dallas, TX), cyclin D1 (SC717; Santa Cruz Biotechnology), phosphorylated Akt (9272; Cell Signaling Technology), and Foxo3a (9476; Cell Signaling Technology). The band intensities were semiquantified by densitometry using Bio-Rad software (Bio-Rad, Hercules, CA).

Statistical Analysis

All experiments were performed at least three times. Quantitative data were presented as mean ± SEM and analyzed by Student *t* test when two groups were compared and analyzed by ANOVA when more than two groups were compared. A P value <0.05 was considered statistically significant.

RESULTS

Fenofibrate Ameliorates Retinal Dysfunction in Diabetic Mice

As quantified by FCM, 6-month-old *db/db* mice showed decreased numbers of ECFC/CACs in the retina, compared with *db/*$^+$ littermate control (CTR) mice (Fig. 1*A*). Interestingly, fenofibrate treatment alleviated the cell number decline in the retina of *db/db* mice compared with the CTR *db/db* mice fed with regular chow (Fig. 1*A*).

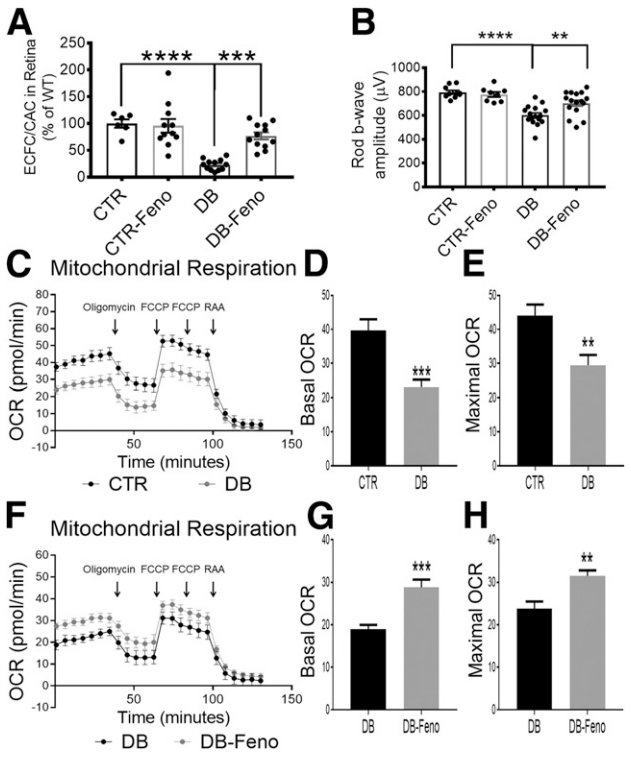

Figure 1—Fenofibrate ameliorated retinal dysfunction and metabolic abnormality in diabetic mice. *A*: *db/db* mice were fed fenofibrate chow starting at 8 weeks of age for 12 weeks. ECFC/CAC numbers in the retina were quantified in *db/db* mice with regular chow (DB), *db/db* with fenofibrate chow (DB-Feno), *db/*$^+$ littermate CTR mice, and CTR with fenofibrate chow (CTR-Feno) ($n = 6$). *B*: Amplitudes of scotopic ERG b-wave in the groups as indicated ($n = 6$). *C*: Measurement of retinal OCR using Seahorse XFe96 analyzer in CTR and *db/db* mice (DB). Basal OCR (*D*) and maximal OCR (*E*) in the retina were measured and compared between *db/db* (DB) and CTR mice ($n > 6$). Measurement and comparison of retinal OCR (*F*) including basal OCR (*G*) and maximal OCR (*H*) in *db/db* mice fed with fenofibrate chow (DB-Feno) and *db/db* mice on regular chow (DB) (mean ± SEM; $^{**}P < 0.01$; $^{***}P < 0.001$; $^{****}P < 0.0001$; $n > 6$). FCCP, carbonyl cyanide-4 (trifluoromethoxy)phenylhydrazone; RAA, rotenone and antimycin A.

As EPCs secrete neurotrophic factors (30), the decreased cell number may contribute to retinal neurodegeneration in DR. Therefore, we examined the retinal function in *db/db* mice using ERG. ERG recording showed that amplitudes of scotopic b-wave declined in *db/db* mice, whereas fenofibrate treatment partially prevented the b-wave decline in *db/db* mice (Fig. 1*B*). Our previous research showed that PPARα has an essential role in retinal lipid metabolism (15); therefore, we used a Seahorse assay to examine whether fenofibrate was able to prevent the mitochondrial dysfunction in the retina of *db/db* mice. Retinal mitochondrial respiration rate was decreased in *db/db* mice compared with CTR mice, as shown by reduced basal and maximal oxygen consumption rate (OCR) (Fig. 1*C–E*). Treatment with fenofibrate improved the retinal mitochondrial OCR in the retina of *db/db* mice (Fig. 1*F–H*).

Fenofibrate Treatment Normalized ECFC/CAC Number and Mitochondrial Function in *db/db* Mice

To evaluate potential effects of fenofibrate on ECFC/CAC generation and release, we quantified ECFC/CACs in the BM and circulation of *db/db* mice fed with and without fenofibrate chow (Fig. 2*A*). Consistent with the number change in the retina, *db/db* mice showed significant decreases of ECFC/CACs in the BM and circulation, and fenofibrate treatment completely normalized cell numbers in the BM (Fig. 2*B* and *C*) and blood (Fig. 2*D*) of *db/db* mice, suggesting that fenofibrate may ameliorate deficiency of ECFC/CAC generation and release under diabetic conditions.

In addition to the cell number, ECFC/CAC mitochondrial function was examined by the measurement of $\Delta\psi_m$, an important parameter of mitochondrial functions. Circulating ECFC/CACs with JC-1 staining were measured by FCM, as JC-1 dye exhibits potential-dependent accumulation in mitochondria, indicated by a fluorescence emission shift from green (529 nm) to red (590 nm). As shown by the red/green fluorescence intensity ratio, the percentage of ECFC/CACs with high $\Delta\psi_m$ decreased in *db/db* mice compared with that in CTR mice (Fig. 2*E*), suggesting a decline of mitochondrial function. However, administration of fenofibrate significantly increased the ECFC/CACs with high $\Delta\psi_m$ in *db/db* mice, suggesting that fenofibrate restored mitochondrial function in *db/db* mice (Fig. 2*F*).

PPARα Played an Essential Role in the Regulation of ECFC/CAC Mitochondrial Function

To elucidate the mechanism by which PPARα regulates ECFC/CAC number and function in vivo, we induced diabetes in *PPARα*$^{-/-}$ mice using STZ. As quantified by FCM, numbers of ECFC/CAC were decreased in the BM, circulation, and retina in diabetic WT and diabetic *PPARα*$^{-/-}$ mice, compared with those in nondiabetic mice. Interestingly, ECFC/CAC numbers in the circulation and retina of diabetic *PPARα*$^{-/-}$ mice showed a further decline compared with that in diabetic WT mice (Fig. 3*A–C*).

We determined the mitochondrial function of ECFC/CACs in diabetic conditions and the regulation role of PPARα. The mitochondrial function of isolated ECFC/CACs in vivo was evaluated by the percentage of cells with high $\Delta\psi_m$. Under diabetic conditions, the percentage of high $\Delta\psi_m$ ECFC/CACs was decreased compared with nondiabetic CTR mice. *PPARα* knockout (KO) further decreased $\Delta\psi_m$ in ECFC/CACs under diabetic conditions (Fig. 3*D* and *E*). Previously, our group has demonstrated that the PPARα protein level was decreased in the retina under diabetic conditions (31). We further examined PPARα expression in the BM, the putative origin of ECFC/CACs. As shown by Western blot analysis, BM PPARα levels were significantly decreased in STZ-induced diabetic mice, compared with that in nondiabetic CTR mice (Fig. 3*F* and *G*), suggesting that the decrease of PPARα in the BM may contribute to the decreased ECFC/CAC number and function and subsequently retinal degeneration in diabetes.

PPARα$^{-/-}$ ECFCs Showed Deficient Function In Vitro

In order to investigate the mechanism by which PPARα regulates ECFC function under diabetic conditions, we isolated, cultured, and further treated mouse BM-originated ECFCs with 4-hydroxynonenal (HNE) to mimic diabetic stress in vitro. Consistent with the observations in diabetic mice, PPARα levels were reduced in isolated ECFCs exposed to HNE (Fig. 4*A* and *B*). In vitro tube formation from WT and *PPARα*$^{-/-}$ ECFCs was disrupted by HNE; however, treatment with fenofibrate rescued the tube formation in WT ECFCs exposed to HNE, but not in *PPARα*$^{-/-}$ ECFCs (Fig. 4*C* and *D*), suggesting that the protective effect of fenofibrate on ECFCs is PPARα dependent. As shown by ECFC migration assay (Fig. 4*E* and *F*) and BrdU incorporation assay (Fig. 4*G*), primary ECFCs from *PPARα*$^{-/-}$ mice showed decreased migration and proliferation, respectively, compared with WT ECFCs, suggesting that PPARα is essential for ECFC proliferation and homing.

Regulation of ECFC Metabolism Profile by PPARα

The energy metabolism pattern is associated with cell fate, especially stem cell fate (32). To determine if the PPARα effects on ECFC cell fate and function are mediated through the regulation of ECFC metabolism, we investigated the function of PPARα in the ECFC metabolism pattern. Using Seahorse analysis, we found that both glycolysis and mitochondrial respiration were decreased in primary ECFCs isolated from *PPARα*$^{-/-}$ mice compared with those from WT mice (Fig. 5*A*). The stressed OCR and extracellular acidification rate (ECAR) were also decreased in *PPARα*$^{-/-}$ ECFCs compared with WT ECFCs (Fig. 5*A* and *B*), indicating that glycolytic and aerobic energy generation in *PPARα*$^{-/-}$ ECFCs failed to increase in response to stress challenge compared with WT ECFCs (Fig. 5*A*, *C*, and *D*). This result suggested that PPARα played an essential role in energy metabolism regulation, especially under the stress condition.

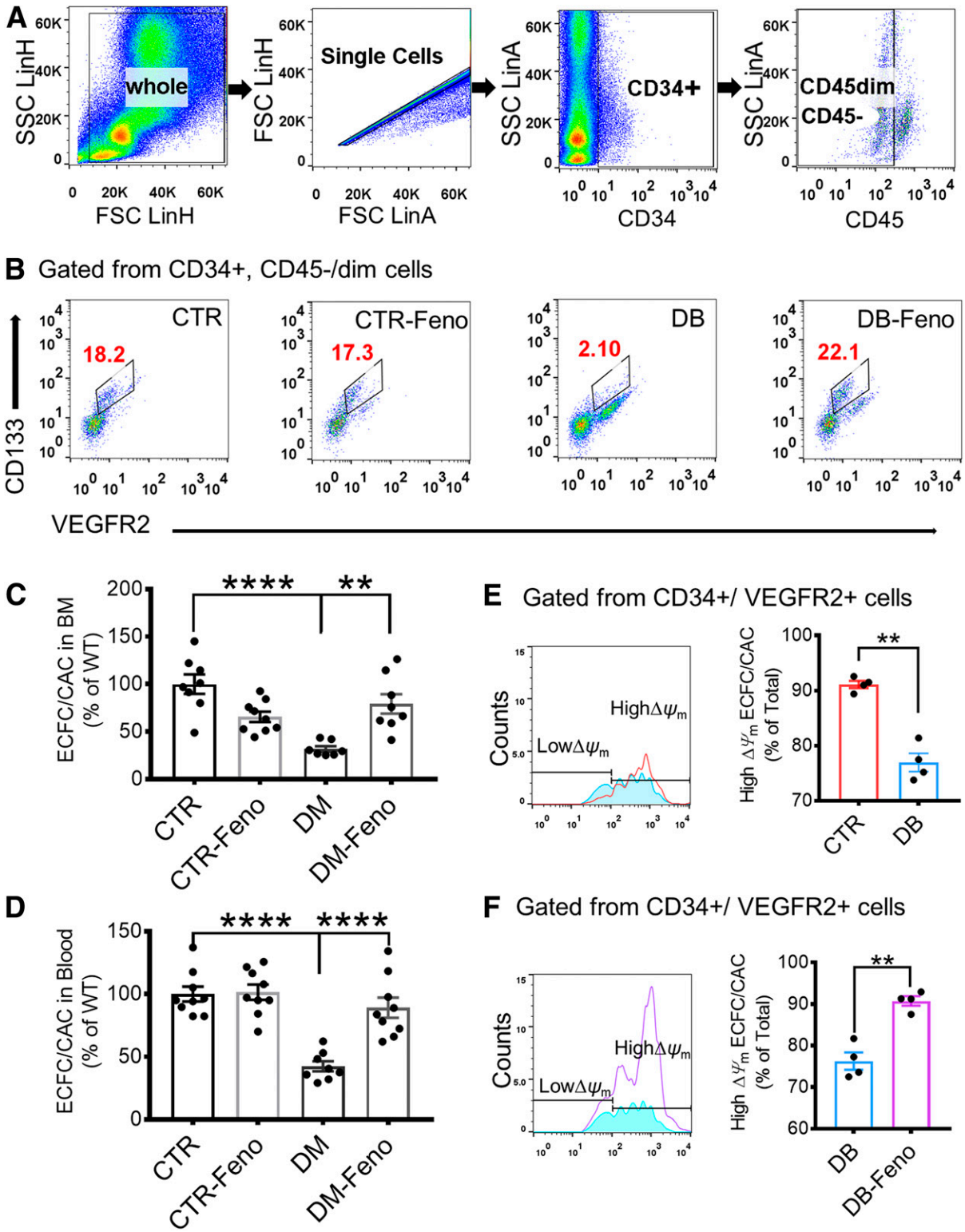

Figure 2— Fenofibrate treatment restored ECFC/CAC number and mitochondrial function in ECFC/CACs in diabetic mice. *A*: Representative FCM gating strategy for the identification of ECFC/CACs ($CD34^+$, $CD45^{-/dim}$, $CD133^+$, $VEGFR2^+$) in the BM. *B*: Representative FCM profiles showed ECFC/CAC number change in the BM of *db/db* mice (DB), *db/db* mice with fenofibrate chow for 12 weeks (DB-Feno), *db/*$^+$ littermate CTR mice, and CTR mice with fenofibrate chow (CTR-Feno). *C*: ECFC/CAC numbers in the BM decreased in *db/db* mice (DB) and were restored by fenofibrate treatment (DB-Feno) ($n = 6$). *D*: ECFC/CAC numbers in the blood decreased in *db/db* mice (DB) and were restored by fenofibrate (DB-Feno) ($n = 5$). *E* and *F*: $\Delta\Psi_m$ was measured by FCM ($n = 4$). *E*: The percentage of ECFC/CACs with high $\Delta\Psi_m$ was decreased in the circulation of *db/db* mice (DB) compared with that in CTR mice ($n = 4$). *F*: Fenofibrate treatment (DB-Feno) elevated the percentage of high $\Delta\Psi_m$ ECFC/CACs in the circulation of *db/db* mice compared with *db/db* mice with regular chow (DB). All values are mean ± SEM. $^{**}P < 0.01$; $^{****}P < 0.001$. FSC, forward light scatter; LinA, linear forward scatter area; LinH, linear forward scatter height; SSC, side scatter.

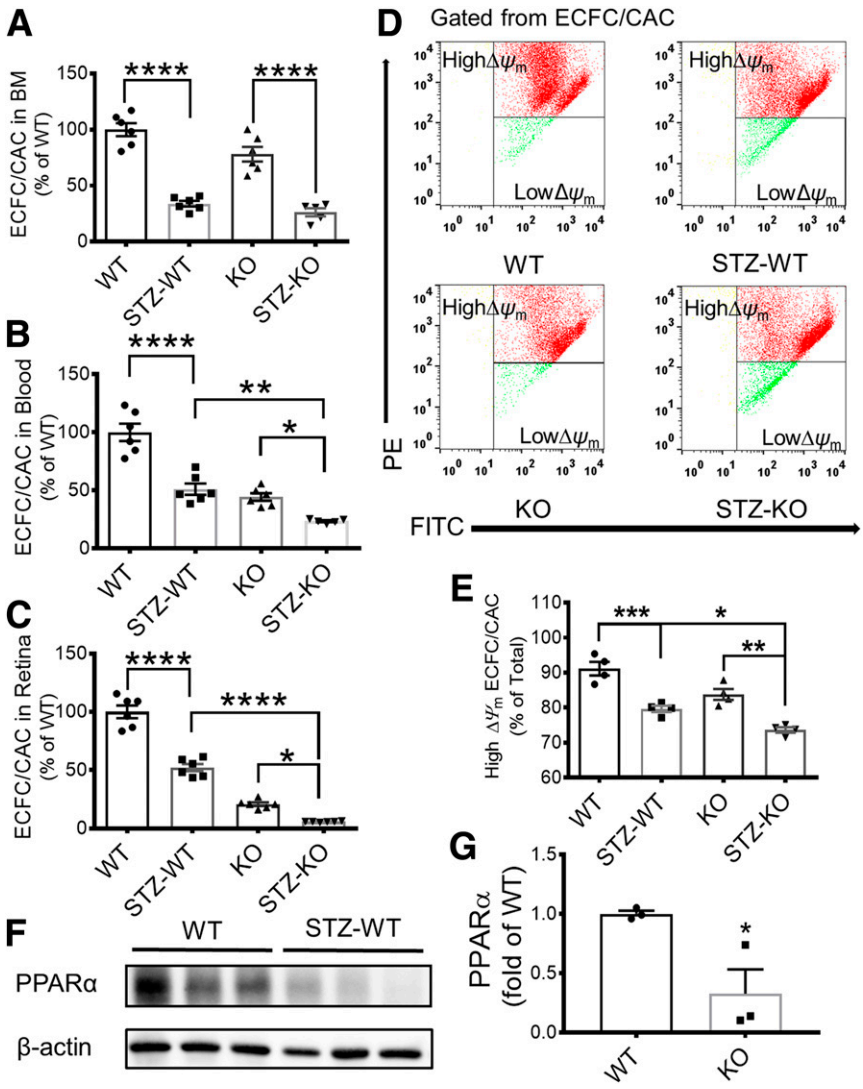

Figure 3—*PPARα* KO decreased ECFC/CAC numbers, homing, and mitochondrial function in diabetic mice. ECFC/CAC numbers were quantified in the BM (*A*), blood (*B*), and retina (*C*) of STZ-induced diabetic WT mice (STZ-WT) at 16 weeks after the onset of diabetes, their age- and genetic background–matched nondiabetic WT mice (WT), STZ-induced diabetic *PPARα*$^{-/-}$ mice (STZ-KO), and nondiabetic *PPARα*$^{-/-}$ mice (KO) ($n = 5$). *D* and *E*: $\Delta\Psi_m$ of ECFC/CACs in the blood was measured by FCM, and the percentage of high $\Delta\Psi_m$ was compared between the groups as indicated. *D*: Representative FCM profiles. *E*: The percentage of high $\Delta\Psi_m$ cells was quantified and compared among the four groups ($n = 4$). Representative Western blots (*F*) and densitometry analyses (*G*) of PPARα protein levels in the BM of WT mice and STZ-induced WT mice (mean ± SEM; *$P < 0.05$; **$P < 0.01$; ***$P < 0.001$; ****$P < 0.0001$). PE, phycoerythrin.

To further determine the role of PPARα in regulating mitochondrial function in ECFC, we measured OCR in isolated ECFCs using a Seahorse XF Cell Mito Stress Test Kit. Under nondiabetic conditions, basal OCR and ATP generation were decreased in *PPARα*$^{-/-}$ ECFCs, compared with that in WT ECFCs (Fig. 5*E–G*). Furthermore, overexpression of PPARα in WT and *PPARα*$^{-/-}$ ECFCs using Ad-PPARα improved the ECFC mitochondrial function, while knockdown of PPARα expression in WT ECFCs using siRNA decreased mitochondrial function (Supplementary Fig. 2), suggesting that PPARα directly contributes to the regulation of ECFC metabolism. The diabetic stressor HNE decreased basal OCR and ATP production in both WT and *PPARα*$^{-/-}$ ECFCs. However, HNE induced more prominent decreases in OCR and ATP production in *PPARα*$^{-/-}$ ECFCs compared with WT ECFCs, suggesting that *PPARα* KO exacerbated mitochondrial dysfunction under diabetic conditions (Fig. 5*E–G*). However, *PPARα* KO did not change total mitochondrial mass in ECFCs (Supplementary Fig. 3).

In addition to mitochondrial respiration, glycolysis is another important metabolic effector to determine stem cell fate and function. Therefore, we determined whether PPARα is also involved in the regulation of glycolysis. The results showed that *PPARα* KO alone decreased basal ECAR, glycolytic capacity ECAR, and glycolytic reserve ECAR, suggesting an impaired glycolytic function in ECFCs in the absence of PPARα (Fig. 6*A–D*). Although HNE

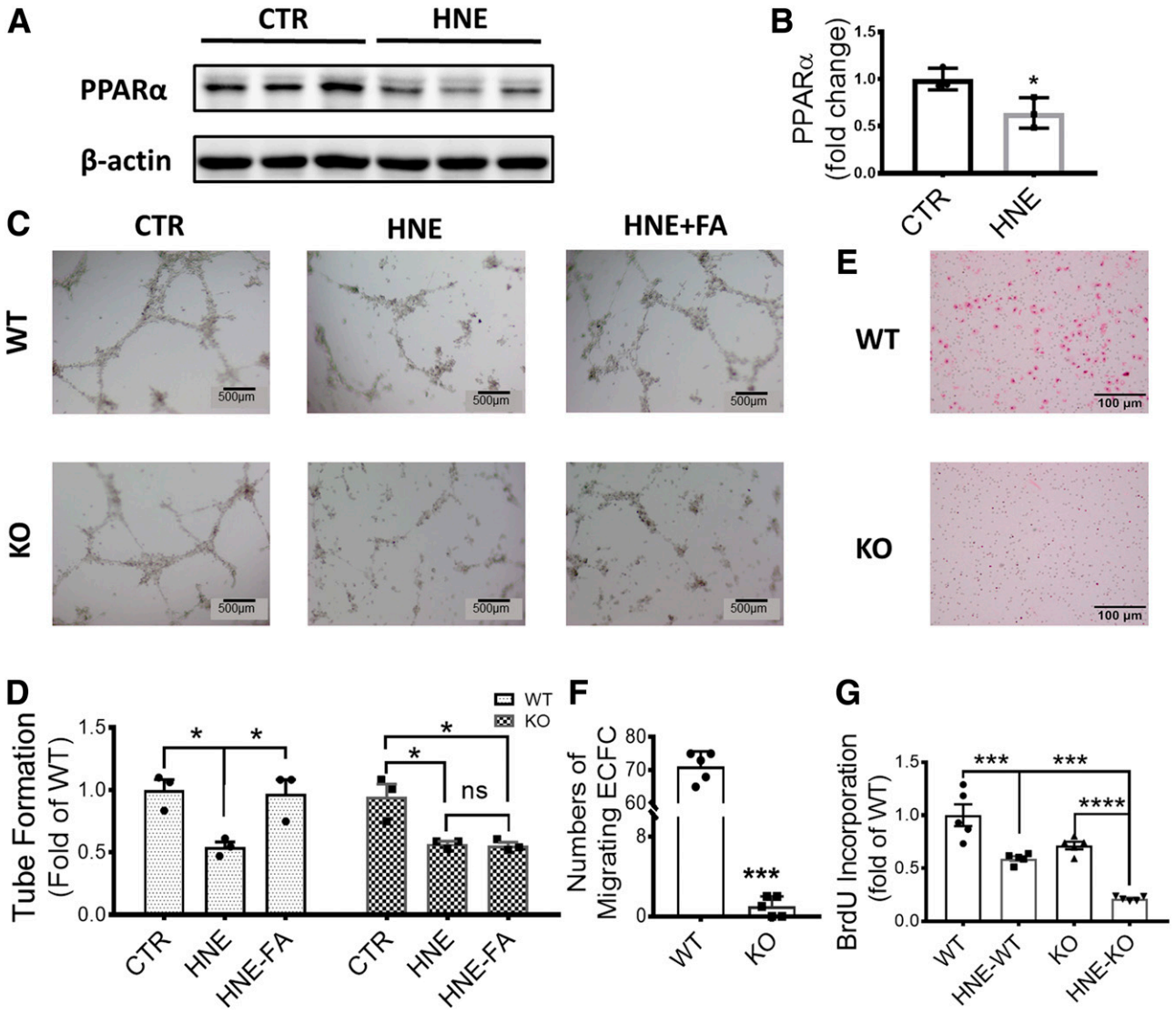

Figure 4—*PPARα* KO impaired ECFC function. Representative Western blots (*A*) and densitometry analyses (*B*) of PPARα protein levels in primary ECFCs treated with HNE (10 μmol/L) and ECFCs treated with vehicle (CTR). *C*: Representative images of in vitro tube formation in WT ECFCs (WT) and *PPARα*$^{-/-}$ ECFCs (KO) treated with HNE and HNE plus fenofibric acid (HNE-FA). *D*: Quantification of tubes formed using ImageJ software ($n = 3$). *E*: Representative micrographs of cell migration transwell assay for WT ECFCs (WT) and *PPARα*$^{-/-}$ ECFCs (KO). The cells that have migrated through the membrane were stained (red) and counted. *F*: Quantification of migrated cells ($n = 3$). *G*: Cell proliferation of ECFCs was analyzed using a BrdU incorporation and BrdU ELISA ($n = 5$). All values are means ± SEM. *$P < 0.05$; ***$P < 0.001$; ****$P < 0.0001$.

treatment for 24 h did not affect glycolytic function in WT ECFCs (Fig. 6*E–H*), it significantly decreased basal ECAR and glycolytic reserve in *PPARα*$^{-/-}$ ECFCs (Fig. 6*I–L*).

Taken together, these results demonstrated that *PPARα* KO decreased mitochondrial oxidation and glycolytic function of ECFCs and further exacerbated diabetic stress–induced damage on these metabolic pathways, especially the mitochondrial function in ECFCs.

PPARα Regulated Akt Phosphorylation to Regulate ECFC Fate and Metabolism

Accumulating evidence suggests that metabolic signaling pathways are strongly associated with the cell cycle. In order to elucidate the mechanism by which PPARα regulates ECFC metabolism and cell fate, we measured the activation of Akt signaling, a master regulator of metabolic pathways. As shown by Western blot analysis, phosphorylated Akt was downregulated in primary *PPARα*$^{-/-}$ ECFCs, compared with that in WT ECFCs. Furthermore, *PPARα*$^{-/-}$ ECFCs also showed reduced levels of downstream factors of Akt signaling, such as Nrf1, Nrf2, Sirt1, and Glut1 (Fig. 7), all of which play important roles in major bioenergetics pathways, including oxidative phosphorylation and glycolysis, and further mediate stem cell proliferation and self-renewal (33–36). Consistently, another target gene of Akt, cyclin D1, an

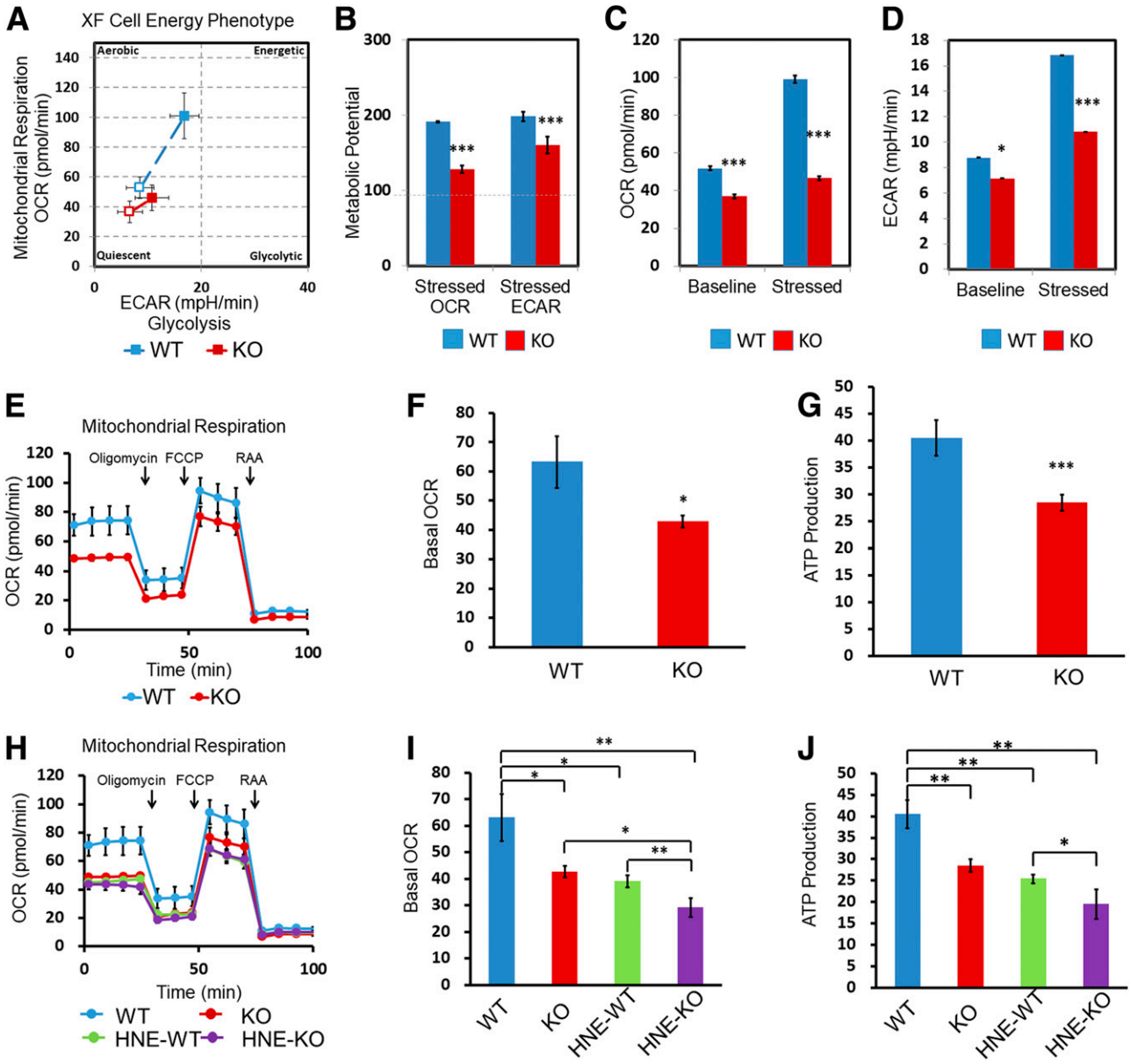

Figure 5—*PPARα* KO decreased ECFC mitochondrial oxidation. *A*: ECFC energy profile was measured and compared between WT ECFCs (WT) and *PPARα*$^{-/-}$ ECFCs (KO); the open square (□) represents baseline metabolism, and filled square (■) represents stressed/maximal metabolism. The distance between the baseline and maximal metabolism represents metabolic potential (*B*), baseline and stressed OCR (*C*), and baseline and stressed ECAR (*D*). *E* and *H*: Representative traces of OCR of WT and KO ECFCs with and without HNE treatment (10 μmol/L, 24 h). The injections of reagents [oligomycin, carbonyl cyanide-4 (trifluoromethoxy)phenylhydrazone (FCCP), and rotenone and antimycin A (RAA)] during the Seahorse analysis are indicated by arrows. Basal OCR (*F* and *I*) and ATP production (*G* and *J*) (the basal respiration that potentially supports ATP production) were calculated and compared. All values are mean ± SEM; $n \geq 3$, $^{*}P < 0.05$; $^{**}P < 0.01$; $^{***}P < 0.001$. mpH, milli pH units.

important G_1 checkpoint protein essential for initiation of the cell cycle, was also downregulated in *PPARα*$^{-/-}$ ECFCs. Taken together, these results suggest that PPARα may regulate energy metabolic pathways in ECFCs through Akt signaling.

DISCUSSION

It has been shown that EPC dysregulation plays important pathogenic roles in diabetic microvascular complications such as DR (7). There are conflicting reports with regard to numbers of circulating EPCs in patients with diabetes (37,38). One explanation is that different cell markers were used in different studies; the other is that the numbers varied during different stages of DR (18). In nonproliferative DR (NPDR), the circulation ECFC/CAC numbers are decreased, while in proliferative DR, the numbers are increased, compared with patients with diabetes without DR (38). However, the pathogenic mechanisms for the dysregulation of ECFC/CAC number and function in diabetes remain elusive. The current study

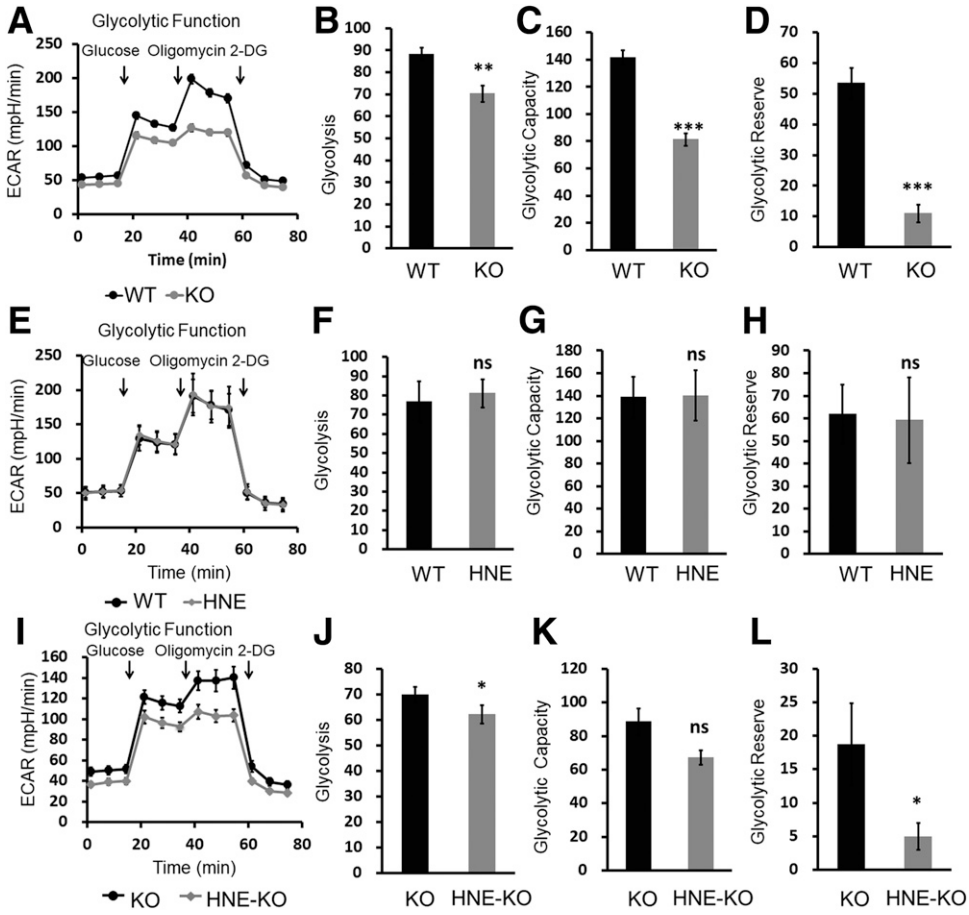

Figure 6—*PPARα* KO decreased ECFC glycolysis. *A*: Injections of reagents (glucose, oligomycin, and 2-deoxyglucose [2-DG]) during Seahorse analysis are indicated by arrows, and their effects on the average ECAR trace were measured in the bioenergetic profile in WT ECFCs (WT) and *PPARα*$^{-/-}$ ECFCs (KO). Glycolysis (*B*), glycolytic capacity (*C*), and glycolytic reserve (*D*) were calculated and compared under nondiabetic conditions. *E*: Representative traces identifying the ECAR of WT ECFCs without (WT) and with HNE treatment (HNE) (10 μmol/L, 24 h). Glycolysis (*F*), glycolytic capacity (*G*), and glycolytic reserve (*H*) were calculated and compared. *I*: Representative traces identifying the ECAR of *PPARα*$^{-/-}$ ECFCs with (HNE-KO) and without (KO) HNE treatment (10 μmol/L, 24 h). Glycolysis (*J*), glycolytic capacity (*K*), and glycolytic reserve (*L*) were calculated and compared under diabetic stress. All values are mean ± SEM; $n \geq 3$. *$P < 0.05$; **$P < 0.01$; ***$P < 0.001$. mpH, milli pH units.

suggests that PPARα plays a key role in the regulation of ECFC/CAC generation, release, and homing, and diabetes-induced PPARα downregulation plays an important role in dysregulation of ECFC/CAC number and function. Further, our study also demonstrates for the first time that PPARα determines ECFC/CAC fate and function through regulating their intrinsic metabolic profile. This study suggests that PPARα in ECFC/CACs is a promising therapeutic target for normalizing vascular repair and regeneration in diabetic conditions, especially in NPDR.

As a type of progenitor cells, ECFCs display two basic characteristics: self-renewal and differentiation (39,40). Self-renewal of ECFCs is essential for maintaining the cell population and stemness, and differentiation refers to cell potency (41). Self-renewal relies more on glycolysis, while differentiation mainly uses mitochondrial oxidative phosphorylation as the metabolism energy source (42,43). In our previous study, we found that *PPARα* KO exacerbates retinal vascular leakage and capillary degeneration under diabetic conditions (31,44). We speculated that ECFC/CAC bioenergetic metabolism might be directly regulated by PPARα, which functions as the nexus of cell maintenance (number change) and repair functions. Hence, we focused on the role of PPARα in the metabolic regulation in ECFC/CACs.

In the current study, we found that ECFC/CACs lose the capacity of maintaining their population in diabetic conditions, not only in the target tissue (retina), but also in the BM and circulation. Consistent with the in vivo results, PPARα deletion exacerbated diabetes stress-induced deficiency in ECFC proliferation and migration. Activation of PPARα using fenofibrate ameliorated the ECFC/CAC population decline in diabetic mice and improved ECFC migration function under diabetic stress. The effect of fenofibrate on ECFC tube formation was abolished by

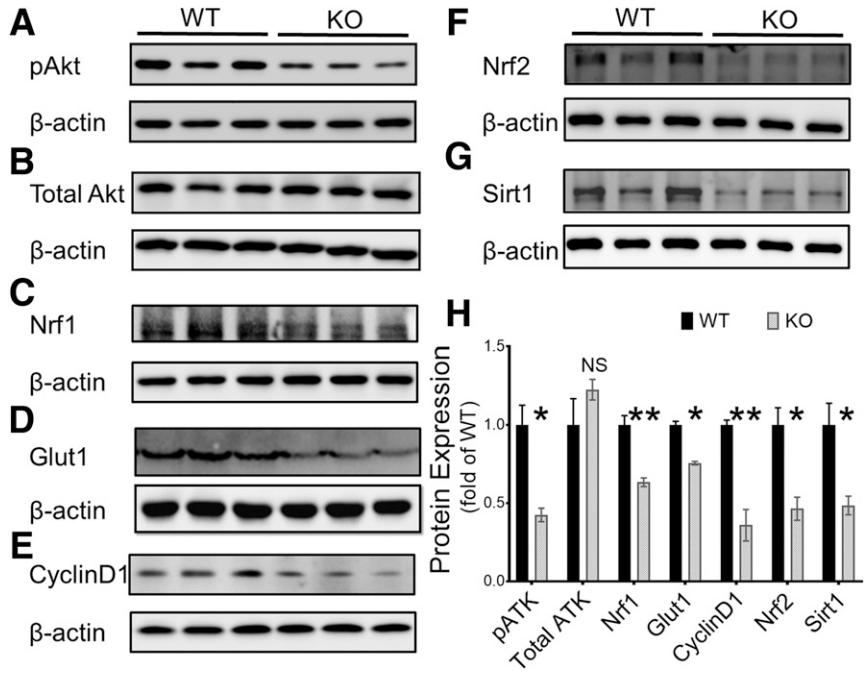

Figure 7—*PPARα* KO decreased Akt activation in ECFCs. *A–G*: Western blot analysis of phosphorylated Akt (pAkt), total Akt, Nrf1, Glut1, cyclin D1, Nrf2, and Sirt1 in primary ECFCs from *PPARα*$^{-/-}$ (KO) and WT mice; β-actin was used as loading control. *H*: Densitometry analysis of protein levels in the Western blots (mean ± SEM; $n = 3$; *$P < 0.05$; **$P < 0.01$).

PPARα ablation, suggesting that the effect of fenofibrate on ECFCs is PPARα dependent.

Previously, we reported that PPARα expression levels decreased in the retinas of patients with diabetes and diabetic animal models (31). The current study demonstrates that PPARα levels are also downregulated in the BM in a diabetic animal model, correlating with the ECFC/CAC population decline in the BM and blood. Further, diabetic stress also downregulated PPARα expression in isolated ECFCs. Because of the function of ECFC/CACs in repairing microvasculature and maintaining vascular integrity, the protective effects of PPARα on ECFC/CACs may explain our previous finding that PPARα activation alleviates the capillary degeneration in the retina of a diabetic model (44).

In addition to vasculogenesis, EPCs also produce neurotrophic factors and thus confer neuroprotective functions (45). Our previous studies reported neuroprotective effects of fenofibrate in a type 1 diabetic animal model (25). Consistently, the current study showed that fenofibrate also alleviated ERG decline in type 2 diabetic mice, suggesting a protective effect on retinal function. The ERG results correlated with the effect of fenofibrate on ECFC/CAC number, suggesting that the neuroprotective effects of fenofibrate in diabetes may be mediated, at least in part, through normalizing ECFC/CAC number and function.

As PPARα functions as an important regulator of cell bioenergetics, this study also investigated if PPARα directly determines ECFC fate under stress or disease conditions. Indeed, Seahorse analysis showed that *PPARα*$^{-/-}$ ECFCs are more quiescent in normal conditions due to less energy usage (glycolysis and FAO). In response to stress, WT ECFCs elevated the OCR and ECAR by ∼100%, while *PPARα*$^{-/-}$ ECFCs only attained a ∼25% increase. These findings suggest that *PPARα*$^{-/-}$ ECFCs have the tendency to remain quiescent and less responsive to external stress, suggesting that the activation of the bioenergetics pathway in response to stress is likely through a PPARα-dependent mechanism.

Cell-intrinsic networks coordinate with signals from the microenvironment to harmonize the self-renewal capacity of stem cells and to maintain homeostasis and activity (46). Most stem cells heavily rely on glycolysis for self-renewal (47) and on FAO for differentiation (42,43). Our results demonstrated that in a diabetic mouse model, the mitochondria of ECFC/CACs showed a decreased $\Delta\Psi_m$, indicating reduced mitochondrial oxidation in vivo. Further, fenofibrate upregulated $\Delta\Psi_m$ in diabetes, while deletion of PPARα exacerbated the $\Delta\Psi_m$ decline in ECFC/CACs under diabetes stress. Our hypothesis is also supported by Seahorse analysis, which showed that not only β-oxidation but also glycolysis is downregulated in *PPARα*$^{-/-}$ ECFCs. This finding clearly demonstrates that PPARα is essential for β-oxidation and glycolysis and facilitates both cell self-renewal and differentiation. In the absence of PPARα, our results suggest that ECFCs remain in a more quiescent state under diabetic conditions. Previous studies showed that quiescent stem cells prefer to stay in the stem cell niche (48) with a decreased homing capacity. This finding is consistent with our

observation that ECFC/CAC numbers decreased in the circulation and retina in *PPARα*$^{-/-}$ mice, but not in the BM. Further, activation and upregulation of PPARα by fenofibrate increased ECFC/CACs in the blood and retina of diabetic mice. All of these results indicate that PPARα is mainly involved in the regulation of ECFC/CAC homing rather than biogenesis. In vitro, the reduced homing capability of *PPARα*$^{-/-}$ ECFCs was demonstrated by their impaired migration function, and decreased differentiation under diabetic conditions was further confirmed by the damaged tube formation.

The Akt pathway has shown protective effects on EPC function in diabetic conditions (49,50). To elucidate the mechanism mediating the effect of PPARα on ECFC metabolism, we measured activation of Akt signaling. *PPARα*$^{-/-}$ ECFCs showed a significantly decreased phosphorylation of Akt, suggesting an impaired activity of the Akt signaling pathway. Consequently, decreased Akt activity in *PPARα*$^{-/-}$ ECFCs resulted in downregulations of a number of Akt downstream responses, such as Nrf2, Nrf1, Sirt1, Glut1, and cyclin D1, etc. All of these downstream factors are actively involved in the regulation of cell survival, proliferation, migration, and differentiation. Nrf2 further regulates the Sirt1 signal pathway to determine human mesenchymal stem cell self-renewal and differentiation (51). Sirt1 is also involved in the regulation of rejuvenation by regulating senescence-associated secretory products (52). Akt activation can also induce the expression of mitochondrial regulator Nrf1 (53), which shares high similarities in structure and function with Nrf2. Glut1 is essential for endothelial cell glucose uptake, which is regulated by the Akt pathway (54). Cyclin D1 is an intrinsic cell cycle checkpoint protein, which can be activated by the Akt pathway (55) and promote cell proliferation (56). Taken together, changed expressions of these Akt target genes highlight an association among PPARα levels, cell metabolism, and cell cycle, at least in ECFCs.

In summary, the current study elucidated a new molecular mechanism by which PPARα regulates ECFC/CAC cell fate and function through directly mediated bioenergetics metabolism via the Akt signaling pathway, especially under diabetic conditions. These findings shed light on new strategies for the treatment of diabetic complications, especially in retinal vascular degeneration in NPDR.

Acknowledgments. The authors thank the Diabetic Animal Core facility and Histology Core facility of Diabetes COBRE for the support and assistance in this study.

Funding. This study was supported by National Institutes of Health grants (EY018659, EY019309, EY012231, EY028949, and GM122744), a JDRF grant (2-SRA-2019-711-S-B), an Oklahoma Center for the Advancement of Science and Technology grant (HR16-041), and a Natural Science Foundation of Tianjin, China, grant (15JCQNJ11400).

Duality of Interest. No potential conflicts of interest relevant to this article were reported.

Author Contributions. Y.S. contributed to the concept, designed and performed the experiments, acquired, analyzed, and interpreted data, and wrote the manuscript. J.C. performed experiments, analyzed and interpreted data, and wrote the manuscript. L.-j.D., X.H., R.C., J.L., and F.Q. performed research, acquired data, and reviewed and edited the manuscript. K.Z. assisted in animal studies. X.-r.L. designed the research and analyzed the data. J.-x.M. designed and directed the study and contributed to writing and editing the manuscript. Y.S., J.C., L.-j.D., X.H., R.C., K.Z., J.L., F.Q., X.-r.L., and J.-x.M. approved the final version of the manuscript. J.-x.M. is the guarantor of this work and, as such, had full access to all of the data in the study and takes responsibility for the integrity of the data and the accuracy of the data analysis.

References

1. Cheung N, Mitchell P, Wong TY. Diabetic retinopathy. Lancet 2010;376:124–136
2. Cade WT. Diabetes-related microvascular and macrovascular diseases in the physical therapy setting. Phys Ther 2008;88:1322–1335
3. Bhatwadekar AD, Duan Y, Korah M, et al. Hematopoietic stem/progenitor involvement in retinal microvascular repair during diabetes: implications for bone marrow rejuvenation. Vision Res 2017;139:211–220
4. Asahara T, Masuda H, Takahashi T, et al. Bone marrow origin of endothelial progenitor cells responsible for postnatal vasculogenesis in physiological and pathological neovascularization. Circ Res 1999;85:221–228
5. Trinh TLP, Li Calzi S, Shaw LC, Yoder MC, Grant MB. Promoting vascular repair in the retina: can stem/progenitor cells help? Eye Brain 2016;8:113–122
6. Banno K, Yoder MC. Tissue regeneration using endothelial colony-forming cells: promising cells for vascular repair. Pediatr Res 2018;83:283–290
7. Lois N, McCarter RV, O'Neill C, Medina RJ, Stitt AW. Endothelial progenitor cells in diabetic retinopathy. Front Endocrinol (Lausanne) 2014;5:44
8. Basile DP, Yoder MC. Circulating and tissue resident endothelial progenitor cells. J Cell Physiol 2014;229:10–16
9. Keech AC, Mitchell P, Summanen PA, et al.; FIELD study investigators. Effect of fenofibrate on the need for laser treatment for diabetic retinopathy (FIELD study): a randomised controlled trial. Lancet 2007;370:1687–1697
10. Chew EY, Ambrosius WT, Davis MD, et al.; ACCORD Study Group; ACCORD Eye Study Group. Effects of medical therapies on retinopathy progression in type 2 diabetes. N Engl J Med 2010;363:233–244
11. Noonan JE, Jenkins AJ, Ma JX, Keech AC, Wang JJ, Lamoureux EL. An update on the molecular actions of fenofibrate and its clinical effects on diabetic retinopathy and other microvascular end points in patients with diabetes. Diabetes 2013;62:3968–3975
12. Deng Y, Han X, Yao Z, et al. PPARα agonist stimulated angiogenesis by improving endothelial precursor cell function via a NLRP3 inflammasome pathway. Cell Physiol Biochem 2017;42:2255–2266
13. Porta N, Vallée L, Lecointe C, et al. Fenofibrate, a peroxisome proliferator-activated receptor-alpha agonist, exerts anticonvulsive properties. Epilepsia 2009;50:943–948
14. Wang YX. PPARs: diverse regulators in energy metabolism and metabolic diseases. Cell Res 2010;20:124–137
15. Pearsall EA, Cheng R, Zhou K, et al. PPARα is essential for retinal lipid metabolism and neuronal survival. BMC Biol 2017;15:113
16. Yamauchi T, Kamon J, Waki H, et al. The fat-derived hormone adiponectin reverses insulin resistance associated with both lipoatrophy and obesity. Nat Med 2001;7:941–946
17. Guerre-Millo M, Gervois P, Raspé E, et al. Peroxisome proliferator-activated receptor alpha activators improve insulin sensitivity and reduce adiposity. J Biol Chem 2000;275:16638–16642
18. Shao Y, Li X, Wood JW, Ma JX. Mitochondrial dysfunctions, endothelial progenitor cells and diabetic retinopathy. J Diabetes Complications 2018;32:966–973
19. Desouza CV, Hamel FG, Bidasee K, O'Connell K. Role of inflammation and insulin resistance in endothelial progenitor cell dysfunction. Diabetes 2011;60:1286–1294
20. Bulhak AA, Jung C, Ostenson CG, Lundberg JO, Sjöquist PO, Pernow J. PPAR-alpha activation protects the type 2 diabetic myocardium against ischemia-

reperfusion injury: involvement of the PI3-Kinase/Akt and NO pathway. Am J Physiol Heart Circ Physiol 2009;296:H719–H727
21. Ravingerová T, Carnická S, Nemčeková M, et al. PPAR-alpha activation as a preconditioning-like intervention in rats in vivo confers myocardial protection against acute ischaemia-reperfusion injury: involvement of PI3K-Akt. Can J Physiol Pharmacol 2012;90:1135–1144
22. Shi Y, Lv X, Liu Y, et al. Elevating ATP-binding cassette transporter G1 improves re-endothelialization function of endothelial progenitor cells via Lyn/Akt/eNOS in diabetic mice. FASEB J 2018;32:6525–6536
23. Peng J, Li Q, Li K, et al. Quercetin improves glucose and lipid metabolism of diabetic rats: involvement of Akt signaling and SIRT1. J Diabetes Res 2017;2017:3417306
24. Wong TY, Simó R, Mitchell P. Fenofibrate - a potential systemic treatment for diabetic retinopathy? Am J Ophthalmol 2012;154:6–12
25. Chen Y, Hu Y, Lin M, et al. Therapeutic effects of PPARα agonists on diabetic retinopathy in type 1 diabetes models. Diabetes 2013;62:261–272
26. Tsukada S, Kwon SM, Matsuda T, et al. Identification of mouse colony-forming endothelial progenitor cells for postnatal neovascularization: a novel insight highlighted by new mouse colony-forming assay. Stem Cell Res Ther 2013;4:20
27. Nagano M, Yamashita T, Hamada H, et al. Identification of functional endothelial progenitor cells suitable for the treatment of ischemic tissue using human umbilical cord blood. Blood 2007;110:151–160
28. Bui KC, Weems M, Biniwale M, et al. Circulating hematopoietic and endothelial progenitor cells in newborn infants: effects of gestational age, postnatal age and clinical stress in the first 3 weeks of life. Early Hum Dev 2013;89:411–418
29. Chen Y, Hu Y, Moiseyev G, Zhou KK, Chen D, Ma JX. Photoreceptor degeneration and retinal inflammation induced by very low-density lipoprotein receptor deficiency. Microvasc Res 2009;78:119–127
30. Rosell A, Morancho A, Navarro-Sobrino M, et al. Factors secreted by endothelial progenitor cells enhance neurorepair responses after cerebral ischemia in mice. PLoS One 2013;8:e73244
31. Hu Y, Chen Y, Ding L, et al. Pathogenic role of diabetes-induced PPAR-α down-regulation in microvascular dysfunction. Proc Natl Acad Sci U S A 2013;110:15401–15406
32. Wanet A, Arnould T, Najimi M, Renard P. Connecting mitochondria, metabolism, and stem cell fate. Stem Cells Dev 2015;24:1957–1971
33. Dinkova-Kostova AT, Abramov AY. The emerging role of Nrf2 in mitochondrial function. Free Radic Biol Med 2015;88:179–188
34. Correia M, Perestrelo T, Rodrigues AS, et al. Sirtuins in metabolism, stemness and differentiation. Biochim biophys acta 2017;1861:3444–3455
35. Chen J, Stahl A, Krah NM, et al. Wnt signaling mediates pathological vascular growth in proliferative retinopathy. Circulation 2011;124:1871–1881
36. Ighodaro I, Eric OK, Adebayo O. Interactions of PPAR α and GLUT4 in DOCA/salt-induced renal injury in mice. Niger J Physiol Sci 2013;28:127–133
37. Lee IG, Chae SL, Kim JC. Involvement of circulating endothelial progenitor cells and vasculogenic factors in the pathogenesis of diabetic retinopathy. Eye (Lond) 2006;20:546–552
38. Brunner S, Schernthaner GH, Satler M, et al. Correlation of different circulating endothelial progenitor cells to stages of diabetic retinopathy: first in vivo data. Invest Ophthalmol Vis Sci 2009;50:392–398
39. Doe CQ. Neural stem cells: balancing self-renewal with differentiation. Development 2008;135:1575–1587
40. Seita J, Weissman IL. Hematopoietic stem cell: self-renewal versus differentiation. Wiley Interdiscip Rev Syst Biol Med 2010;2:640–653
41. Orford KW, Scadden DT. Deconstructing stem cell self-renewal: genetic insights into cell-cycle regulation. Nat Rev Genet 2008;9:115–128
42. Folmes CD, Dzeja PP, Nelson TJ, Terzic A. Mitochondria in control of cell fate. Circ Res 2012;110:526–529
43. Shao Y, Li X, Wood JW, Ma JX. Mitochondrial dysfunctions, endothelial progenitor cells and diabetic retinopathy. J Diabetes Complications 2018;32:966–973
44. Ding L, Cheng R, Hu Y, et al. Peroxisome proliferator-activated receptor α protects capillary pericytes in the retina. Am J Pathol 2014;184:2709–2720
45. Liu X, Li Y, Liu Y, et al. Endothelial progenitor cells (EPCs) mobilized and activated by neurotrophic factors may contribute to pathologic neovascularization in diabetic retinopathy. Am J Pathol 2010;176:504–515
46. Simons BD, Clevers H. Strategies for homeostatic stem cell self-renewal in adult tissues. Cell 2011;145:851–862
47. Ito K, Suda T. Metabolic requirements for the maintenance of self-renewing stem cells. Nat Rev Mol Cell Biol 2014;15:243–256
48. Arai F, Suda T. Quiescent stem cells in the niche. In *StemBook*. Cambridge, MA, Harvard Stem Cell Institute, 2008
49. Dai X, Yan X, Zeng J, et al. Elevating CXCR7 improves angiogenic function of EPCs via Akt/GSK-3β/fyn-mediated Nrf2 activation in diabetic limb ischemia. Circ Res 2017;120:e7–e23
50. Wang RY, Liu LH, Liu H, et al. Nrf2 protects against diabetic dysfunction of endothelial progenitor cells via regulating cell senescence. Int J Mol Med 2018 42:1327–1340
51. Chen Y, Hu Y, Zhou T, et al. Activation of the Wnt pathway plays a pathogenic role in diabetic retinopathy in humans and animal models. Am J Pathol 2009;175:2676–2685
52. Goligorsky MS. Endothelial progenitor cells: from senescence to rejuvenation. Semin Nephrol 2014;34:365–373
53. Jovaisaite V, Mouchiroud L, Auwerx J. The mitochondrial unfolded protein response, a conserved stress response pathway with implications in health and disease. J Exp Biol 2014;217:137–143
54. Melstrom LG, Salabat MR, Ding XZ, et al. Apigenin inhibits the GLUT-1 glucose transporter and the phosphoinositide 3-kinase/Akt pathway in human pancreatic cancer cells. Pancreas 2008;37:426–431
55. Muise-Helmericks RC, Grimes HL, Bellacosa A, Malstrom SE, Tsichlis PN, Rosen N. Cyclin D expression is controlled post-transcriptionally via a phosphatidylinositol 3-kinase/Akt-dependent pathway. J Biol Chem 1998;273:29864–29872
56. Qiu C, Xie Q, Zhang D, Chen Q, Hu J, Xu L. GM-CSF induces cyclin D1 expression and proliferation of endothelial progenitor cells via PI3K and MAPK signaling. Cell Physiol Biochem 2014;33:784–795